Atomic force microscopy study of the growth and annealing of Ge islands on Si(100)

Bing Liu, Cindy L. Berrie, Takeshi Kitajima, John Bright, and Stephen R. Leone[a)]
JILA, University of Colorado and National Institute of Standards and Technology, and Department of Chemistry and Biochemistry and Department of Physics, University of Colorado, Boulder, Colorado 80309-0440

(Received 24 October 2001; accepted for publication 21 January 2002)

Atomic force microscopy is used to study the growth and annealing of Ge islands on Si(100) by molecular beam epitaxy. The Ge island shape, size distribution, number density, and spatial distribution under various growth conditions, such as different substrate temperatures, Ge beam fluxes, and annealing times, are investigated. By limiting the growth to a low coverage of 6 ML of Ge, we find that either a low growth temperature ($\leq$875 K) or a high beam flux can produce films dominated by pyramids of {105} facets. Domes of higher aspect ratios only appear at high growth temperatures or after a long time of annealing at low temperatures. This indicates that in the competition between the different kinetic processes responsible for the pyramid and dome formation, the domes require a higher activation energy and grow slower. We also demonstrate that appropriate annealing at low temperature can form locally ordered arrays of pyramids with a narrow size distribution. © *2002 American Vacuum Society.* [DOI: 10.1116/1.1459724]

I. INTRODUCTION

Growth of Ge on Si is a classical example of the Stranski–Krastanov (SK) growth mode, i.e., a wetting layer of several monolayer (ML) thickness [3–5 ML for Ge/Si(100)] is followed by formation of three-dimensional (3D) islands. Smaller than a certain size, the 3D Ge islands on Si are coherently strained (dislocation free),[1] and therefore the growth processes are potentially applicable to the fabrication of device-quality self-assembled quantum dots. In previous studies,[2–4] two types of coherent Ge islands on Si(100) have been observed, differing in both size and shape. They are pyramids bounded by four {105} facets, and domes of steeper and complex facets [e.g., {113} and {102}]. During growth, Ge islands first appear as pyramids. When reaching a certain size, the pyramids change shape to become domes.[5]

In order to explain the bimodal size distribution and the shape transition of Ge/Si(100) islands, Ross *et al.*[5] studied the dependence of the chemical potential on island shape and size. They proposed that, at a certain size, the chemical potential of an island of a high aspect ratio becomes lower than that of an island of a low aspect ratio, and an island shape transition occurs as a first order phase transition. After the transition, similar to the case of the classical Ostwald ripening, the steeper islands will grow larger at the expense of the smaller and flatter islands.

Several processes have been suggested to contribute to the pyramid to dome transition. Corners of a pyramid could first start to dissolve because of their sharp curvatures.[6] The atoms at the island edge could disassociate because of the high local strain.[7,8] Si–Ge intermixing will also help to relieve the strain,[8–11] and as a result both types of islands obtain higher contents of Si and larger volumes.[9]

On the other hand, Kamins *et al.*[12] (>900 K) observed that, during annealing of Ge/Si(100) islands at high temperatures, a dome island could change its shape back to a pyramid. They suggested that both shapes (i.e., pyramid and dome) are stable structures for coherent Ge/Si(100) islands.

For the fabrication of self-assembled quantum dots, it is desirable to have a narrow island size distribution. It is apparent that the bimodal size distribution of Ge islands on Si(100) is an impediment to this goal. It is worthwhile to study additional aspects of the growth kinetics of pyramids and domes, so that we may find appropriate conditions to control the growth to obtain a stable ensemble of islands of only one type and a narrow size distribution.

In the present work, using atomic force microscopy (AFM) and growth by molecular beam epitaxy (MBE), we first study the morphology dependence of Ge islands on Si(100) as a function of growth temperature and beam flux. Differing from many previous studies of Ge/Si(100) islands, our growth experiments are limited to a low coverage of 6 monolayers (MLs), which is just above the critical thickness for the SK growth of Ge/Si(100). At higher coverages, islands can become large enough to relax through dislocations.[13,14] A dislocated island will grow very fast to become a very large, relaxed "superdome" (named by Williams *et al.*[15]). Superdomes will not only consume most of the supersaturation, but also the surrounding small coherent islands.[16] This complicates the interpretation of island density and size distribution.

In the second part of this work, we study the effect of low temperature annealing on the morphology and 2D (lateral) ordering of the islands. It has been suggested that the film strain favors the formation of periodic domains[17,18] (e.g., arrays of islands). Lateral ordering of coherent islands has been observed previously in InAs/GaAs heteroepitaxy.[19,20] However, contradictory results were also obtained for this system.

[a)]Author to whom correspondence should be addressed: srl@jila.colorado.edu; National Institute of Standards and Technology.

Based on comparisons between an experimental observation of the spatial distribution of InAs/GaAs islands and a computer simulation, Leonard *et al.*[21] pointed out that the spatial distribution of the islands is actually random. In the Ge/Si system, lateral ordering of Ge islands in Si/Ge superlattice structures[22] and on highly stepped Si surfaces[23] have been reported. In our growth of a single layer of Ge islands on Si(100), analysis of the nearest neighbor distances and orientations indicate that appropriate annealing indeed can introduce a level of 2D ordering and a narrower island size distribution.

II. EXPERIMENT

All growth experiments were performed in a home-built MBE chamber with a base pressure in the 1×10^{-10} Torr (10^{-8} Pa) range. The chamber is equipped with an Auger electron spectrometer, reflection high energy diffraction (RHEED), a quartz crystal microbalance, and a radiative sample heater. The growth system and the substrate cleaning procedure are described in detail elsewhere.[24] Samples were grown at surface temperatures varied in intervals of: (a) 25 K from 800 to 900 K and (b) 50 K from 900 to 1000 K. The flux was kept constant (1 ML/min) for the study of the temperature dependence of growth. A few samples were grown at a flux of 10 ML/min for comparisons of the growth kinetics. The total coverage of Ge is 6 ML for all the samples. After growth, the samples were either cooled to room temperature quickly by switching off the heater or left for annealing at the growth temperature for a specific amount of time.

The surface morphology was measured *ex situ* by AFM in tapping mode. All samples were imaged quickly after removal from vacuum so that the basic island shapes can be resolved by AFM. In the AFM images taken a few days later, the island shapes became less clear, which is probably due to the native oxidation of the samples. A special program was developed by the authors to measure the size (height, radius, and volume) and shape of the Ge islands. The basic island shapes observed in this work are consistent with previously reported *in situ* scanning tunneling microscopy observations.[2,3] This confirms that, for the relatively large sizes of the Ge islands studied here, our data are valid and within the accuracy afforded by the AFM tip sizes. To ensure good statistics, AFM images were taken at different places on the samples and the total number of islands measured for each sample varied from several hundred to more than 2000.

III. RESULTS AND DISCUSSION

A. Growth of 6 ML of Ge on Si(100) at different substrate temperatures without annealing

Figures 1(a) and 1(b) show typical AFM images of the samples grown at 850 and 950 K. The corresponding island aspect ratio plots (height versus full width) are shown in Figs. 1(c) and 1(d). The islands in Fig. 1(a) have an average full width (measured along the [100] direction) of 32 nm and an average height of 2.2 nm, corresponding to an aspect ratio

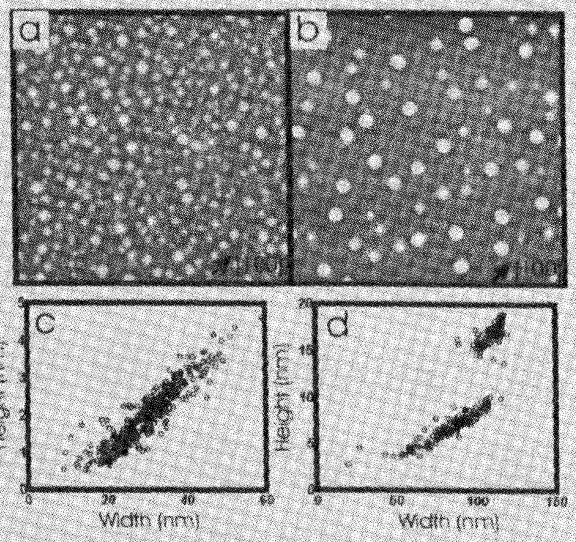

FIG. 1. AFM images and aspect ratio plots (height vs full width) of 6 ML Ge grown on Si(100) at 850 K (a), (c), and 950 K (b), (d). The image sizes are 1×1 μm^2 (a) and 2×2 μm^2 (b). Black and white contractions are 10 nm for the vertical scale for both images. The bimodal size distribution is clear in (d). The aspect ratio plots include more points than shown in the corresponding images.

(height over half width) of 0.14. If we remove the AFM tip effect by simply subtracting the radius of curvature of the tip (about 5 nm in our experiments) from the average island width, this result is consistent with that of pyramids composed of {105} facets with the bases oriented along the ⟨100⟩ directions. [The pyramidal island shape is more evident in the statistics of the island surface normal vectors, which will be exemplified in Fig. 4(c)]. At 950 K, dome islands that have larger sizes and higher aspect ratios appear as round and larger features in the AFM images [Fig. 1(b)]. A bimodal size distribution is apparent in the plot of Fig. 1(d). These results are consistent with previous observations.[3–5]

Figures 2(a) and 2(b) show details of the temperature dependence of the island morphologies. Figure 2(a) is the island volume as a function of the growth temperature. Below 875 K, the pyramid volume increases slowly with temperature and there are no dome islands. Above 875 K, domes appear and coexist with pyramids, and the volumes of both types of islands increase faster than below 875 K.

In general, assuming the total coverage and the beam flux are constants, because of the temperature-enhanced adatom surface diffusion, a higher substrate temperature would produce larger islands (with a lower density). However, previous studies of the temperature dependence of Ge islands on Si(100) provide contradictory observations. Goryll *et al.*[25] observed three types of islands, i.e., pyramids, domes, and superdomes for growth temperatures ranging from 825 to 975 K. They found that only the average volume of the superdomes increases with temperature, while the two smaller types of coherent islands do not grow with temperature. One possible reason for this difference with our observation may be the low coverage we used. As introduced in Sec. I, at a higher coverage (about 37 ML of Ge on Si in the work of

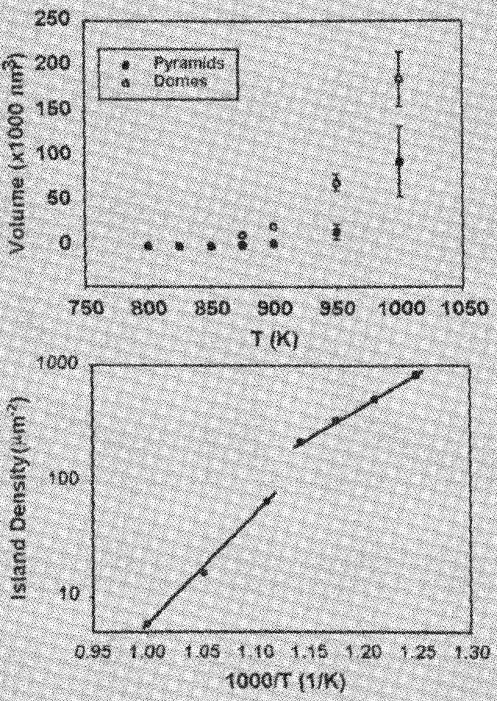

FIG. 2. Temperature dependence of (a) average Ge island volume and (b) Ge island density (number of islands per unit area), where pyramids and domes are counted together. Note from (a) that domes do not appear below 875 K, and above that temperature, the island density decreases faster with increasing temperature (b).

Goryll *et al.*[25]), some large islands may relax through dislocations and then grow very fast to become superdomes. Consequently, the growth of the coherent islands would be suppressed because of the presence of the superdomes that consume a large fraction of the supersaturation.

Capellini *et al.*[9] reported an increase of the Ge/Si(100) island size with growth temperature, ranging from 775 to 1125 K, without making distinctions between the two types of coherent islands. Our observation [Fig. 2(a)] is consistent with their report, which indicates that the average Ge island size starts to increase faster as the temperature is raised above 875 K. With x-ray photoelectron spectroscopy measurements of the Ge/Si islands,[9] Capellini *et al.* also found that the Si content in the islands increases with the same trend as the average island volume does with the temperature. This means that, in addition to the effect of the temperature-enhanced adatom surface diffusion, Si–Ge intermixing also plays a role in the increase of the island volumes.

Figure 2(b) shows the temperature dependence of the island density (where the pyramids and the domes are counted together). It is apparent that, above 875 K, the island density decreases faster with increasing temperature than below 875 K. This can be explained partly by the appearance of the dome islands at these temperatures. The domes are larger than the pyramids, therefore fewer islands are formed. In addition, in our experiments, by observing the time when the 2×1 streaky RHEED patterns change to bright spots (which indicates the appearance of 3D islands), we notice that with the constant deposition rate of 1 ML/min, at temperatures above 875 K, it takes a longer time (about 5–6 min of deposition) for the 2D–3D transition to happen, whereas at low temperatures, the transition takes less time (about 3–4 min of deposition). This implies that there is a thicker wetting layer and less Ge is available for the 3D islands at high temperatures. This could also contribute to the more rapid decrease in the island density at high temperatures. Indeed previous studies of the growth of Ge on Si(100)[26] have found that, even for submonolayer deposition, a substrate temperature of 875 K can enhance Si–Ge intermixing, which would lower the strain energy of the growing film and allow formation of a thicker wetting layer.

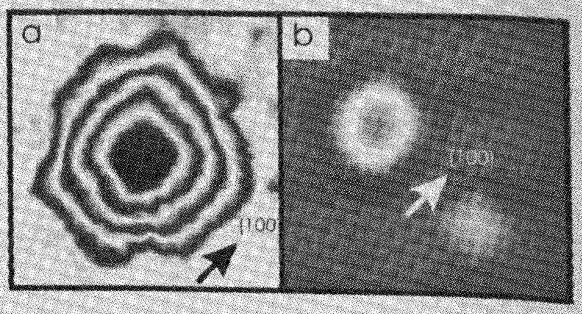

FIG. 3. Two examples of the processes of dome formation: (a) dissolving of a pyramid's corners, displayed as a contour plot with contour interval of 3.3 nm; the island height is 15 nm; (b) formation of trenches (the dark areas) around the dome island, roughly oriented along the [100] directions). In (b), the dome island is 37 nm high and the pyramid is 10 nm high. The image sizes are 0.2×0.2 μm^2 (a) and 0.4×0.4 μm^2 (b).

Regarding the mechanisms of dome formation, because the pyramid edges are highly strained, the appearance of the domes could be a result of the strain-enhanced Si–Ge intermixing that starts first around the pyramid edges.[8] In addition to this, we observe some real instances of dome formation in our experiments. Figure 3(a) catches an island at an intermediate stage between a pyramid and a dome. It shows that the top of the island still has a pyramidal shape while the corners have already started to dissolve. Because the island corners have larger curvatures than the edges, it is more likely for atoms to detach from the corners. Ultimately, this process would proceed until the sharp corners become round.

Figure 3(b), showing a dome and a pyramid, is an instance of another process. The dark regions around the dome are deeper than the flat interisland wetting layer. They are indicative of trenches around the dome edges. From cross-sectional measurements, we find that there are no clear trenches around the pyramids, which suggests that the trenches occur along with the dome formation. Trenches have been reported before to occur around Ge/Si(100) domes.[27] In addition to previously reported characteristics, our results show that they are oriented along the (100) directions. We note that the trench depth can be greater than the generally agreed upon value of the thickness of the Ge/Si(100) wetting layer (about 3–5 ML), which implies that this process can extend into the Si substrate, and consequently, the content of Si in the domes would be increased

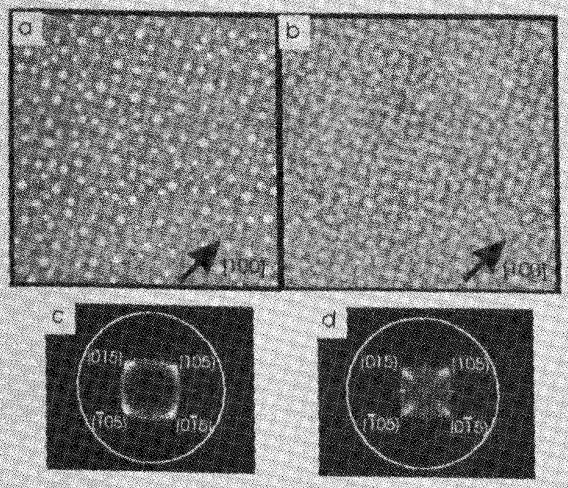

FIG. 4. AFM images (a), (b) and histograms of the surface normal of the island facets (c), (d) of Ge pyramids grown by a deposition of 6 ML Ge on Si(100) with a flux of 10 ML/min at 950 K without annealing (a), (c), and a flux of 1 ML/min and annealed for 100 min at 800 K (b), (d). The image sizes are 2×2 μm^2 for (a) and 1×1 μm^2 for (b). The island surface normal histograms are plotted in polar coordinates, with the polar angle measured with respect to the [110] direction, and the distance to the origin represents the angle measured with respect to the [001] direction.

equivalently because part of the Si substrate is depleted to supply material to the dome formation and, at the island base, more Si is exposed to become a part of the island.

In these experiments, because of the low flux (1 ML/min) and the low coverage (6 ML) which produce relatively low island densities, we rule out the possibility of dome formation by coalescence of pyramids, which would be more significant at higher coverages (≥8 ML) and higher beam fluxes (≥3 ML/min).[16]

Note that the processes involved in the dome formation (e.g., Si–Ge intermixing, dissolving of the pyramid corners, and trench formation) all involve breaking Ge–Ge, Si–Si, and Ge–Si bonds. They may require higher activation energies than nucleation of islands that involves diffusion and attachment. Hence, the dome formation is significant only at high temperatures and would occur slower than nucleation of pyramids. This speculation is confirmed by growth experiments with a high flux at 950 K and by annealing experiments at lower temperatures, as discussed next.

Figure 4(a) shows an AFM image of islands of 6 ML Ge on Si(100) grown at 950 K with a high beam flux of 10 ML/min, which requires a deposition time of only 36 s. The islands are dominated by pyramids, as evidenced by the histogram of the island surface normal plot of Fig. 4(c), where four peaks of contact angle of 12° along the (100) directions are apparent, and they correspond to the four {105} facets of the pyramids.[2,3] Compared with Fig. 1(b), which is a sample with the same Ge coverage and grown at the same temperature but with a much lower beam flux (1 ML/min), it is clear that, even at this high temperature, the nucleation of pyramids can still dominate the island growth. Figure 4(b) is a case at low substrate temperature. It is a sample of 6 ML Ge grown at 800 K (the flux is 1 ML/min) and annealed at the same temperature for 100 min. Figure 4(d) is the histogram plot of the island surface normals of this sample. Apparently, at this low temperature, pyramids can dominate the island population for a long time. As a last example, Figs. 5(a)–5(c) (which will be discussed in detail in the next section) show the results of a series of annealing experiments on several samples at 825 K. At this temperature, domes finally appear after annealing for 400 min [see Fig. 5(c), where the {113} facets of the domes are evident in the surface normal plot of Fig. 5(f)].

As a summary of this part, in these experiments of MBE growth of Ge on Si(100), we reproduce the previously reported bimodal island size distributions and island shape identifications. We also find that in the competition between the different mechanisms responsible for the formation of the two types of islands, the processes for pyramid formation are faster than those for the dome production at a given temperature. Therefore, using different beam fluxes, we can control the growth kinetics so that an ensemble of islands composed of only pyramids can be obtained at both low and high growth temperatures.

B. Effects of low temperature annealing on the island morphology

Annealing experiments are very important for studying the evolution of island morphology. In general, unless the deposition rate is much lower than the corresponding rates of surface diffusion and island formation, after the deposition is complete, the islands will still evolve unless the heating of the substrate is turned off. During annealing, kinetic processes such as ripening take effect and the ensemble of islands evolve to equilibrium.

As an example, consider the series of annealing experiments briefly mentioned in Sec. III A. Figures 5(a)–5(c) are AFM images of three samples of 6 ML Ge grown on Si(100) at 825 K in 6 min. The times of annealing at 825 K are t_a = 0, 40, and 400 min, respectively. Figures 5(d)–5(f) are the statistics of the island surface normals, and Figs. 5(g)–5(i) show the measured island volume distribution of the three samples, respectively. The islands evolve from their morphology right after deposition [t_a = 0 min, see Figs. 5(a), 5(d), and 5(g)] to an ensemble of larger pyramids [t_a = 40 min, see Figs. 5(b), 5(e), and 5(h)]. Note the change in image size between 5(a) and 5(b). After a long annealing time of 400 min, domes finally appear [Figs. 5(c), 5(f), and 5(i)]. We discuss the three samples one by one to consider the possible effects of low temperature annealing.

For the first sample with no annealing (t_a = 0), since the total time of growth is short, we consider the island distribution of this sample as a result of nucleation with negligible ripening. The solid line in the plot of its volume distribution [Fig. 5(g)] is a fit to a lognormal distribution.[28] The reason we choose this function for the fit is that the volume distribution has a long tail toward large values, and it has been shown that, at the nucleation stage, a lognormal function can well represent the island size distribution.

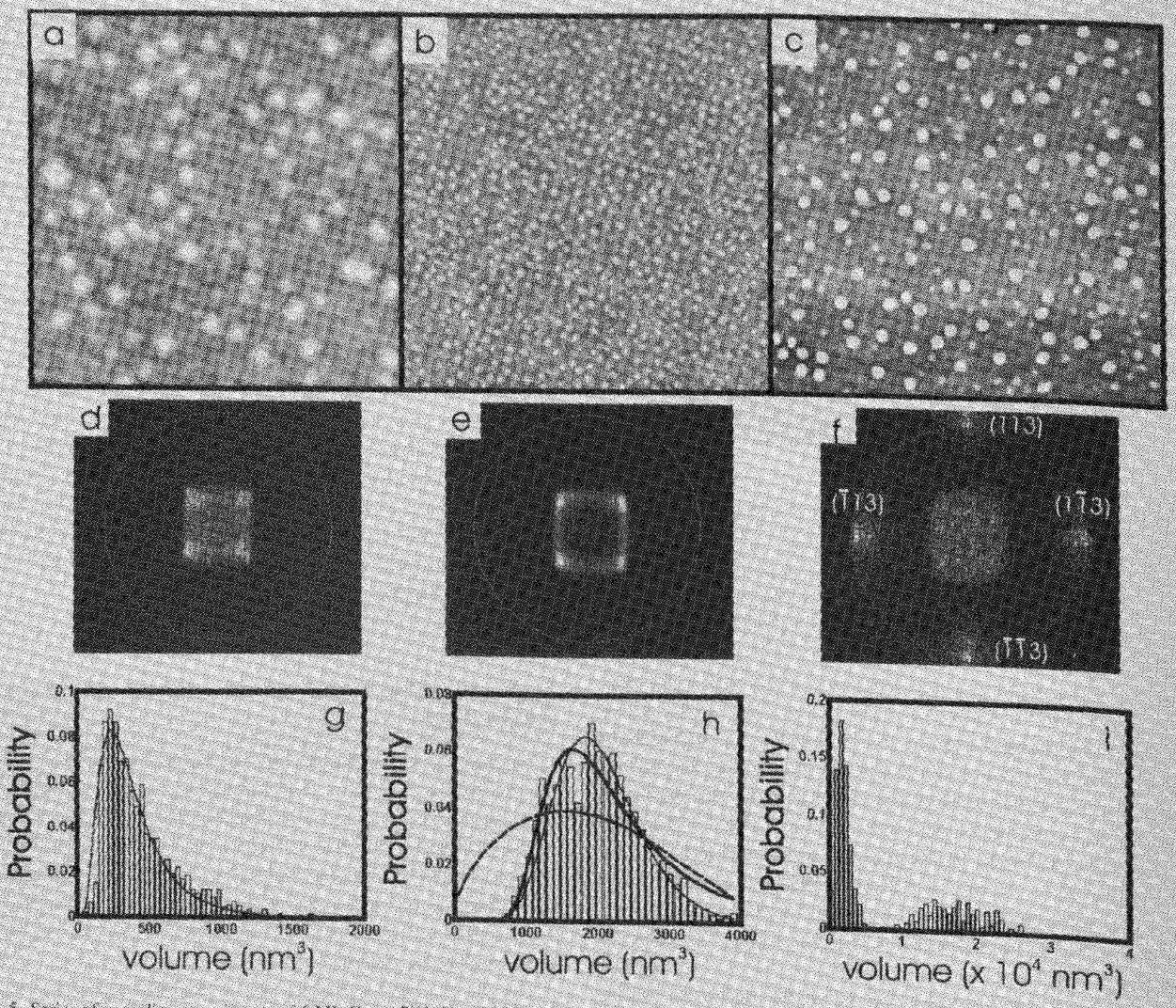

FIG. 5. Series of annealing experiments of 6 ML Ge on Si(100) at 825 K: (a) after deposition of 6 min with an annealing time of zero (0.5×0.5 μm^2); (b) after annealing for 40 min (2×2 μm^2); and (c) after annealing for 400 min, where domes finally appear (2×2 μm^2). The black and white contraction of the vertical scale is 40 nm. (d)–(f) are the corresponding surface normal statistics. The {113} facets of the domes are observed in (f) as the four peaks on the circle of 26°. (g)–(i) are island volume distributions. The solid line in (g) is a lognormal fit. In (h), the thin solid line is a fit to the modified model by Tersoff and Tromp; the thick solid line is a fit to Shchukin's model; and the dashed line is a fit to a theoretical ripening distribution.

Now consider the second sample with $t_a=40$ min. It is interesting to note that, for this sample, the islands are not only still dominated by pyramids, but they also seem to have more uniform size, shape, and spatial distributions than without annealing. The ratio of the standard deviation of island volume over the mean island volume for this sample is about 0.4, while for the sample with no annealing (i.e., the sample with $t_a=0$), this value is about 0.9. The uniformity of the island shape is reflected in the surface normal statistics. Figure 5(e) shows sharper peaks of the {105} facets than Fig. 5(d).

The spatial distribution of the islands of this sample is also worth noting. As introduced in Sec. I, it was predicted that, for heteroepitaxial films, the strain relaxation prefers formation of periodic domains (e.g., arrays of islands). This effect has been studied for III–V material systems[19–21] and Ge/Si superlattice structures.[22] In our experiments, lateral ordering of the pyramids is observed. For this sample with $t_a=40$ min, the degree of ordering is characterized by the statistics of the nearest neighbor center-to-center distances [translational ordering, see Fig. 6(a)] and the nearest neighbor pair directions [orientational ordering, see Fig. 6(b)]. There is evidence that both probability distributions strongly peak at a few values, suggesting a level of local ordering.

One question is whether this is still just a case of a random distribution of clusters, which could also show some ordering, especially at high densities (i.e., random close packing).[29] To verify this, we performed a computer simulation of a random distribution of an ensemble of rectangular 2D clusters. To ensure the same area coverage of islands, the ensemble of the 2D clusters in the simulation have the same size distribution and the same total number as the measured ensemble of pyramids. The simulation result [dashed line in Fig. 6(a)] follows the envelope of the peaks of the measured

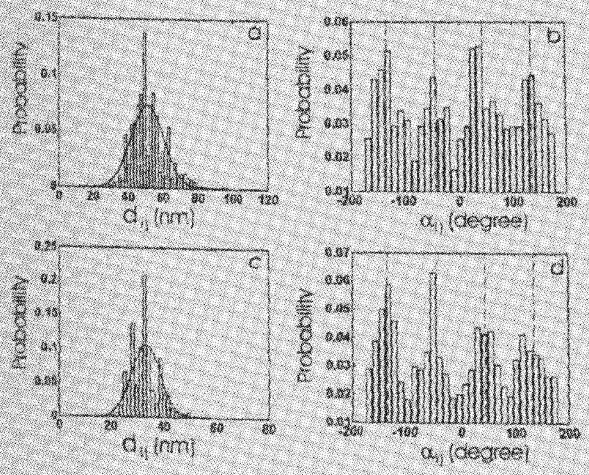

FIG. 6. (a), (c) Distribution of the nearest neighbor center-to-center distance d_{ij}, and (b), (d) the nearest neighbor pair direction angles α_{ij} measured with respect to the [110] direction for two samples of 6 ML Ge grown and annealed at 825 K for 40 min (a), (b), and 800 K for 100 min (c), (d). The dashed lines in (a) and (c) are results of computer simulation of random distribution. The dashed lines in (b) and (d) represent perfect orientational ordering along the ⟨100⟩ directions.

distribution of the nearest neighbor distances, but it does not reproduce the very prominent central peak. Thus the ordering effect observed here is more than a random close packing.

Figures 6(c) and 6(d) show another example, this time 6 ML Ge grown on Si(100) in 6 min and annealed for 100 min at 800 K. [Refer to Fig. 4(a) for the corresponding AFM image.] These results also suggest translational [Fig. 6(c)] and orientational [Fig. 6(d)] ordering.

The reason for the ordering of pyramids most likely lies in the elastic interaction (repelling forces) between them,[17,18] which make the whole ensemble of islands become an interconnected network. In the theoretical study by Shchukin *et al.*,[30] the energy of arrays of pyramids on a cubic (100) surface is calculated, and it was found that there may exist an energy minimum where arrays of pyramids can be stable against further evolution. According to this, in the case of Ge islands on Si(100), formation of pyramids may not be just a kinetically favored process because an ordered array of pyramids can be a local equilibrium.

Assuming that the ordered arrays of Ge/Si(100) pyramids we observed are close to the local equilibrium as suggested by Shchukin *et al.*, the island size (volume) would then take on an approximate Boltzmann distribution, i.e., $p = p_0 \exp(-\mathcal{E}(V)/kT)$, where $\mathcal{E}(V)$ is the island energy per unit volume as a function of the volume (V). In previous studies, the free energy of coherent islands of different shapes has been obtained in this way.[2] The thick solid line in Fig. 5(h) is a least squares fit to the experimental island volume distribution using Shchukin's model.[30]

Tersoff and Tromp[31] also calculated the energy of a single strained island. We modified their model by setting the geometry factors to that of the pyramids bounded by four {105} planes (i.e., aspect ratio of 0.2 and contact angle of 11°) and explicitly included an approximate expression for the elastic interaction energy between two strained islands as $E_{\text{inter}} = CV_iV_j/d_{ij}^3$,[30] where V_i and V_j are neighboring island volumes; d_{ij} is the distance between the two islands, and C is a combination of elastic constants. The thin solid line in Fig. 5(h) is a least squares fit to this model.

Since from the nucleation stage to the state of uniformly distributed pyramids, the islands undergo ripening, we also compared the experimental results with two theoretical distributions of ripening at steady state, i.e., attachment/detachment limited mass transport[32] [dashed line in Fig. 5(h)] and diffusion limited mass transport (the classical Ostwald ripening,[33] not shown here).

For the two types of theoretical models above (i.e., two thermodynamic ones and two kinetic ones), we conclude that the experimental agreement is much better with the thermodynamic models, which emphasizes the importance of the role of the elastic interactions between the islands.

Finally, we consider the last sample in this series of annealing in Fig. 5(c) at $t_a = 400$ min. After this long time of annealing, domes finally appear [Fig. 5(c)]. The {113} facets are evidenced in the surface normal plots [Fig. 5(f)]. The size distribution becomes bimodal [Fig. 5(i)]. This confirms one of the conclusions of Sec. III A, i.e., the processes of dome formation are slower compared to the formation of pyramids. It is worth mentioning that the final island density of this sample is much lower than the sample with $t_a = 40$ min, which implies that pyramids start to disappear after the appearance of domes. Those pyramids are possibly dissolved and contribute to the growth of the domes. This is qualitatively in agreement with the modified Ostwald ripening proposed by Ross *et al.*[5]

IV. CONCLUSIONS

We performed a systematic study of the early stage of growth of Ge on Si(100) by MBE at a low coverage of 6 ML. Analysis of the experimental results demonstrate that: (i) for an ensemble of islands of medium or low densities, the dome formation requires a higher activation energy; it is therefore possible, by controlling the growth kinetics, to obtain Ge islands that are composed of only pyramids at both low and high temperatures; (ii) due to the elastic interaction between strained islands, ordered arrays of pyramids can be established in a local equilibrium, which can be reached through appropriate low temperature annealing, and the pyramids are more uniform in shape and size than those without annealing. These results are important to the fabrication of self-assembled quantum dots of desired size, shape, and spatial distributions.

ACKNOWLEDGMENTS

The authors are grateful for the financial support from the National Institute of Standards Technology and the National Science Foundation. J.B. thanks the National Science Foundation Research Experiences for Undergraduates Program for support.

[1]D. J. Eaglesham and M. Cerullo, Phys. Rev. Lett. **64**, 1943 (1990).
[2]Y.-W. Mo, D. E. Savage, B. S. Swartzentruber, and M. G. Lagally, Phys. Rev. Lett. **65**, 1020 (1990).
[3]G. Medeiros-Ribeiro, A. M. Bratkovski, T. I. Kamins, D. A. A. Ohlberg, and R. S. Williams, Science **279**, 353 (1998), and references therein.
[4]F. M. Ross, R. M. Tromp, and M. C. Reuter, Science **286**, 1931 (1999), and references therein.
[5]F. M. Ross, J. Tersoff, and R. M. Tromp, Phys. Rev. Lett. **80**, 984 (1998).
[6]T. I. Kamins and R. S. Williams, Surf. Sci. **405**, L580 (1998).
[7]A.-L. Barabasi, Appl. Phys. Lett. **70**, 2565 (1997).
[8]S. A. Chaparro, J. Drucker, Y. Zhang, D. Chandrasekhar, M. R. McCartney, and D. J. Smith, Phys. Rev. Lett. **83**, 1199 (1999).
[9]G. Capellini, M. De Seta, and F. Evangelisti, Appl. Phys. Lett. **78**, 303 (2001).
[10]J. Walz, T. Hesjedal, E. Chilla, and R. Koch, Appl. Phys. A: Mater. Sci. Process. **69**, 467 (1999).
[11]X. Z. Liao, J. Zou, D. J. H. Cockayne, J. Qin, Z. M. Jiao, X. Wang, and R. Leon, Phys. Rev. Lett. **83**, 1399 (1999).
[12]T. I. Kamins, G. Medeiros-Ribeiro, D. A. A. Ohlberg, and R. S. Williams, Appl. Phys. A: Mater. Sci. Process. **67**, 727 (1998).
[13]M. Hammar, F. K. LeGoues, J. Tersoff, M. C. Reuter, and R. M. Tromp, Surf. Sci. **349**, 129 (1996).
[14]Y. Hirovama and M. Tamura, J. Vac. Sci. Technol. A **16**, 2956 (1998).
[15]R. S. Williams, G. Medeiros-Ribeiro, T. I. Kamins, and D. A. A. Ohlberg, J. Phys. Chem. B **102**, 9605 (1998).
[16]We have performed a series of growth experiments to study growth of Ge on Si(100) at high coverages and beam fluxes. The results will be submitted elsewhere.
[17]D. Vanderbilt, Surf. Sci. **268**, L300 (1992).
[18]P. Zeppenfeld, M. Krzyzowski, C. Romainczuk, G. Comsa, and M. G. Lagally, Phys. Rev. Lett. **72**, 2737 (1994).
[19]J. M. Moison, F. Houzay, F. Barthe, L. Leprince, E. Andre, and O. Vatel, Appl. Phys. Lett. **64**, 196 (1994).
[20]S. Ruvimov *et al.*, Phys. Rev. B **51**, 14766 (1995).
[21]D. Leonard, S. Fafard, K. Pond, Y. H. Zhang, J. L. Merz, and P. M. Petroff, J. Vac. Sci. Technol. B **12**, 2516 (1994).
[22]J. Tersoff, C. Teichert, and M. G. Lagally, Phys. Rev. Lett. **76**, 1675 (1996).
[23]J. Zhu, K. Brunner, and G. Abstreiter, Appl. Phys. Lett. **73**, 620 (1998).
[24]C. L. Berrie, B. Liu, and S. R. Leone, Appl. Surf. Sci. **175**, 69 (2001).
[25]M. Goryll, L. Vescan, K. Schmidt, S. Mesters, H. Luth, and K. Szot, Appl. Phys. Lett. **71**, 410 (1997).
[26]L. Patthey, E. L. Bullock, T. Abukawa, S. Kono, and L. S. O. Johansson, Phys. Rev. Lett. **75**, 2538 (1995).
[27]S. A. Chaparro, Y. Zhang, and J. Drucker, Appl. Phys. Lett. **76**, 3534 (2000).
[28]C. G. Grandqvist and R. A. Buhrman, Appl. Phys. Lett. **27**, 693 (1975).
[29]Y. L. Duparcmeur, J. P. Troadec, and A. Gervois, J. Phys. I **7**, 1181 (1997).
[30]V. A. Shchukin, N. N. Ledentsov, P. S. Kop'ev, and D. Bimberg, Phys. Rev. Lett. **75**, 2968 (1995).
[31]J. Tersoff and R. M. Tromp, Phys. Rev. Lett. **70**, 2782 (1993).
[32]M. Iwamatsu and Y. Okabe, J. Appl. Phys. **86**, 5541 (1999).
[33]B. K. Chakraverty, J. Phys. Chem. Solids **28**, 2401 (1967).